Large scale simulation of optical-material interaction to determine laser ablation in liquid and spectral absorptivity of perfect light absorber

Sy-Bor Wen, Arun Bhaskar, Kevin Ly

Department of Mechanical Engineering, Texas A&M University, College Station, TX 77843

Introduction

A range of important physical mechanisms can happen when light strikes a surface. For example, absorption and transmission of light can happen at the surface, which can result in heating of the target either at the surface or beneath the surface depending on the absorption coefficient of the target and the focusing behavior of the light. The optically induced heating, when it is strong enough, can cause mass removal from the target with micron (or even sub-micron) scale precision. With this high level of precision, optical based bio-surgeries and high precision micron fabrications become popular in recent decades. The absorption behavior of light at the surface can be tweaked through material selection and the microscale patterns fabricated on the surface. It is recently reported that perfect light absorbers at selected one or multiple wavelengths can be achieved when appropriate patterns which can induce both electric and magnetic field resonances are fabricated on the surface. Such new types of surface structures are valuable in radiative energy detection and harvest for different renewable energy applications. In this poster, we summarized a portion of our previous work relating to the utilization of wave optics to determine the optical–material interactions and the associated joule heating/ phase change behavior of the material. The presentation is divided into two portions, namely, (a) optical induced vapor bubble formation/expansion in water-like bio-tissues. Such phenomenon is called micro-cavitation in bio-tissues, and is important in a wide range of laser-surgeries; (b) design of multiband perfect light absorbers (at near-IR wavelength). Such design is important in the development of high sensitivity IR sensors as well as near IR energy harvesters. Since Maxwell's equations are applied to handle the wave type simulations, required mesh size should be equal or less than ~λ/4 to ~λ/10. More than a few millions of meshes are commonly required in each simulation. Therefore, we mainly rely on Ada clusters at TAMU especially for cases requiring parametric sweeped parallel simulations.

Theory

The numerical results presented in the following sections are based on solving the following governing equations under 2D evolutionarily symmetric or 3D conditions with either finite different finite element method (FEM).

(a) Wave optical simulation with Maxwell's equations in frequency domain

$$\nabla\cdot\vec{D}=0;\qquad \nabla\cdot\vec{B}=0;\qquad \nabla\times\vec{E}=-j\omega\mu_o\vec{H};\qquad \nabla\times\vec{H}=j\omega\varepsilon_r\varepsilon_o\vec{E}$$

where $\vec{E}$, $\vec{D}$, $\vec{B}$ and $\vec{H}$ are the electric field, electric displacement, magnetic induction and magnetic field in the frequency domains; ε_r is the relative permittivity of the material, ε_o is the permittivity of free space; μ_o is the permeability of the material. The induced current density is $\vec{J}=j\omega\vec{D}$. The time average joule heating Φ is equal to $1/2\,\mathrm{Re}(-j\omega E\cdot D^*)$.

(b) Mass conservation simulation for solid/liquid/vapor phases

$$\frac{\partial\rho}{\partial t}=-\nabla\cdot(\rho\vec{V})$$

where ρ is the local density of the simulation field.

(c) Momentum conversation simulation with stress from strain field (solid phase) or strain rate field (liquid/vapor phase)

$$\rho\frac{\partial\vec{V}}{\partial t}+\rho(\vec{V}\cdot\nabla)\vec{V}=\nabla\cdot\vec{\vec{\sigma}}+\vec{F}_b\qquad \frac{\partial\vec{u}}{\partial t}+(\vec{V}\cdot\nabla)\vec{u}=\vec{V}$$

where $\vec{V}$ is the velocity field; $\vec{\vec{\sigma}}$ is the stress tensor; $\vec{u}$ is the displacement field. For solid phase, the stress tensor is related to the strain field with linear elastic theory. For liquid/vapor phases, the stress tensor is related to the strain rate field with Newtonian fluid assumptions.

(d) Heat transfer simulation with two temperature model for the heat diffusion in the solid/liquid/vapor phases

$$C_e\frac{\partial T_e}{\partial t}=\Phi+\nabla\cdot(\kappa_e\nabla T_e)-\frac{C_e}{\tau_{e-p}}(T_e-T_p)\qquad C_p\frac{\partial T_p}{\partial t}=\nabla\cdot(\kappa_p\nabla T_p)+\frac{C_p}{\tau_{e-p}}(T_e-T_p)$$

where C_e and C_p are the heat capacity of electrons and phonons, respectively; T_e and T_p are the electron and phonon temperatures, respectively; and κ_e are $\kappa_p$electron and phonon conductivity, respectively; and τ_{e-p} is the relaxation time between the electrons and phonons. Φ the laser induced heating rate. To reduce the simulation time, the wave optics simulation is decoupled with the heat transfer analysis, which is a good assumption when the light pulse width is much less than the thermal diffusion time constant.

(e) Equation of state for liquid/vapor phases

$$P=\frac{RT}{\tilde{v}-\tilde{b}}-\frac{a(T)}{\tilde{v}^2+2\tilde{b}\tilde{v}-\tilde{b}^2};\ a(T)=0.45724\frac{(RT_c)^2}{P_c}\left[1+m(1-\sqrt{T_r})\right]^2;$$

$$m=0.37464+1.5422\varpi-0.26992\varpi^2;\ T_r=\frac{T}{T_c};\ \tilde{b}=0.0778\frac{RT_c}{P_c};\ \tilde{v}=v+c$$

As a first order of approximation, we assume the equation of state of tissue is the same as water when it is in the liquid or vapor phase.

(f) Internal energy, e, and specific heat, C_p

With equation of state, we can determined internal energy e with

$$\left(\frac{\partial e}{\partial v}\right)_T=\left[T\left(\frac{\partial P}{\partial T}\right)_v-P\right]$$

The specific heat is then determined from

$$C_p=\rho c_p=\rho\left(\frac{\partial e}{\partial T}\right)_p=fct(T,p)$$

Optically induced vapor bubble in water

The simulation of optically induced vapor bubble in water as well as its expansion process can be divided into two stages. First, we simulate a flattop laser light delivered to a water-like target through a hemispherical lens. The resulting joule heating in the target especially around the focal point can be estimated from

$$Joule\ heating=\frac{1}{2}\langle\vec{J}\cdot\vec{E}\rangle$$

with $\vec{J}$ the induced current.

The obtained joule heating rate per unit volume from the full wave simulation is then inserted into the energy equation as the Φ term to determine the induced heating. The temperature increment of the target during the EM joule heating induces the deformation, velocity fields, and phase change of the target, which can described with conversation equations and equation of state of the target. To properly handle the deformation of the target due to the expansion of the vapor bubble, arbitrary Lagrangian-Eulerian (ALE) method and moving meshes to trace the movement of the top boundary is adopted. The obtained results are listed in the following figures 1-4.

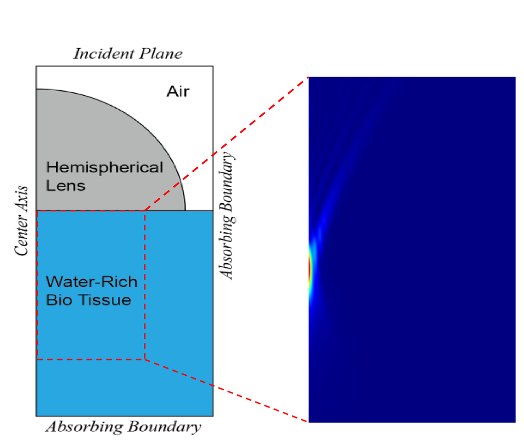

Figure 1. (a) Simulation domain for the plane wave propagation through a hemispherical lens and then focus inside the bio tissue. (b) Spatial distribution of joule heating inside the bio tissue. A rainbow color scale is applied to illustrate the relative intensity value. The domain size of the joule-heating plot is 100 µm x 150 µm

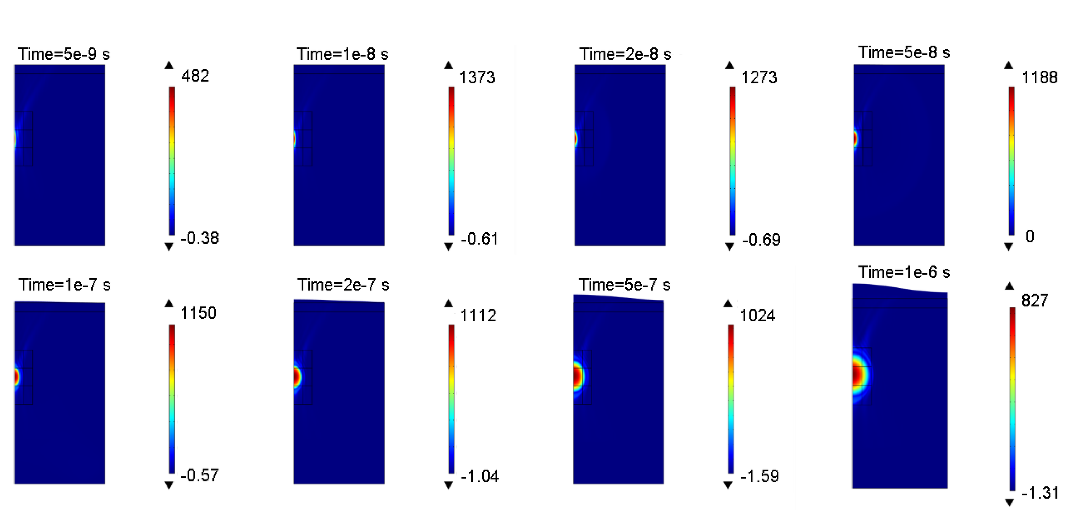

Figure 2. Temperature increment (on top of 293.15 K with unit of Kelvin) inside the water-like target at different delay times from the beginning of the 10 ns laser pulse.

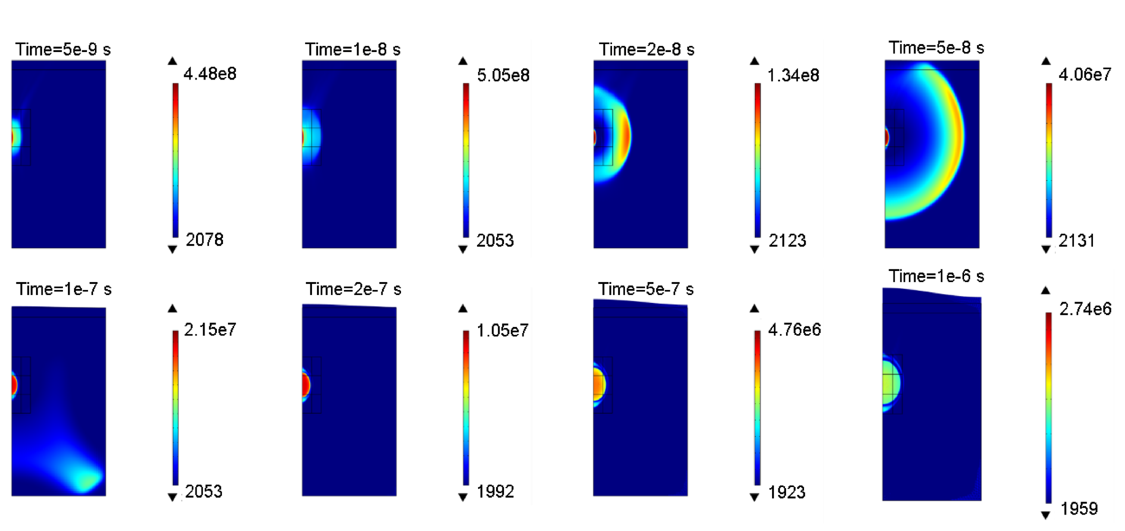

Figure 3. Pressure distribution (with unit of Pa) inside the water-like target at different delay times. A spherical shockwave wave detaches from the focal spot at the end of the laser pulse (i.e., 10 ns)

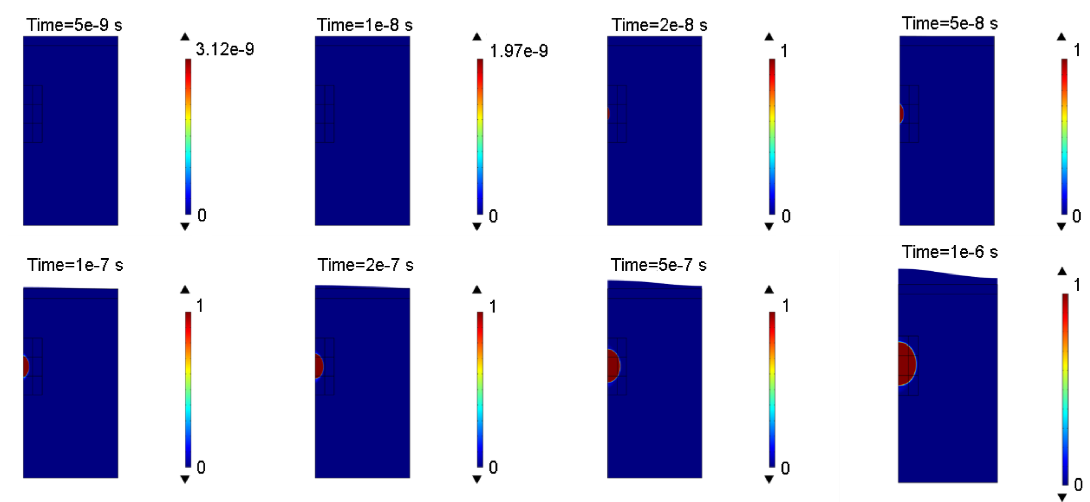

Figure 4. Vapor quality (i.e., mass fraction of vapor at each local position) inside the water-like target at different delay times. Vapor quality equals one (i.e., red color region of the figure) when the local material is fully converted into vapor phase.

Figure 1 shows the joule heating rate inside a the target around the laser spot. The incident laser energy is 0.02 mJ with a pulse duration ~10 ns and wavelength ~4 µm. The absorption coefficient of water-like tissue is ~8759 m^{-1} at this specific wavelength. The laser spot with a diameter ~4 µm is located at ~120 µm beneath the surface of the target through the top hemispherical lens. Figure 2 shows the evolution of the temperature increment inside the target (on top of ambient temperature at 300 K) during and after the laser pulse. Based on figure 2, the maximum temperature increment (~1373 K) happens at the end of the laser pulse. The heat affected zone increases monotonically after the laser pulse due to the thermal diffusion, which causes pressure increment of the target. Figure 3 shows the pressure field due to the heating effect. The rapid pressure rise during the laser pulse owing the joule heating induces a spherical shockwave with high speed. The shockwave passes through the 100 µm x 200 µm simulation domain in ~100 ns. Figure 4 shows the vapor qualify of the target due to the phase change caused by the high temperature and pressure around the focal spot. Rapid phase change happens at ~40 ns after the laser pulse. This time delay can be attributed to the required time for pressure release from the focal spot and the resulting phase change. As illustrated as the red region of figure 4, the vaporized material gradually forms a spherical vapor bubble during the expansion process. The appearance of the vapor bubble also causes swelling of the water-like target from the top boundary, which is captured with our ALE and moving mesh method. Through repeating similar simulations under different laser energy, wavelength, and pulse duration, we are able to characterize the laser induced microcavitation process as a function of laser conditions, which is important in different types of laser surgeries.

Design of multiband perfect light absorber

A perfect light absorber is a device which absorbs all the energy that is incident upon it at a particular wavelength. A perfect absorber can be achieved with metamaterial composed with micro/nanoscale surface patterns. It was shown in a previous study that perfect light absorber could be realized using a gold cross electric ring resonator (ERR) separated from a conducting gold layer using a thin Gallium Antimonide dielectric layer. When light with appropriate wavelength strikes the metal cross-shape ERR, standing electric field with high intensity will be induced in the ERR, which will in turn causes strong magnetic field resonance in the dielectric layer confined by the top metallic ERR and the bottom metal base. By adjusting the amplitude of the electric and magnetic resonance, the impedance of the metamaterial can be fine tuned to provide zero reflection at selected wavelengths (i.e., perfect absorber). To achieve this critical condition for perfect light absorption, the size of each ERR and the thickness of the dielectric layer should be well designed. To determine the required size of the ERR when it is made with Au as well as the required thickness of the dielectric layer to achieve perfect light absorption at specific wavelength, we have to carry out a parametric sweep simulation, using full wave simulation based on Maxwell's equation to test the light absorptivity of this specific type of metamaterial with different sizes of Au cross-shaped ERR and different dielectric layer thickness with full wave simulation. Figure AA shows the simulation domain and the results are presented in figures 5 for design of metasurface absorbers providing perfect light absorption at λ~6.5µm with alumina as the dielectric layer.

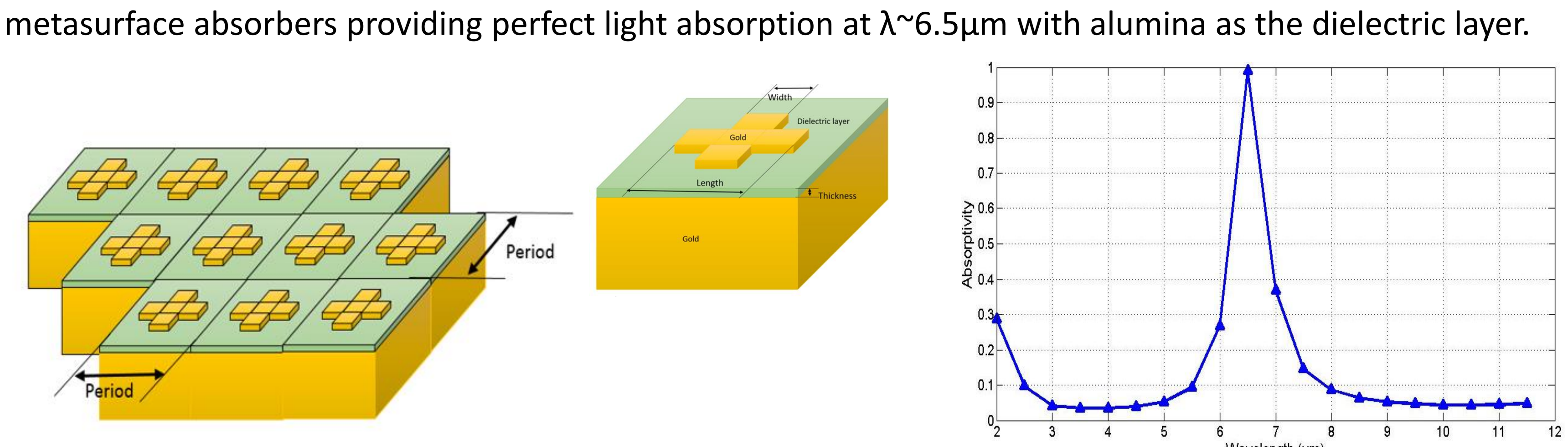

Figure 5. (a) an infinitely large array of electric ring resonators (ERR) on top of a thin dielectric layer (in green color); (b) A unit cell of the metasurface absorber; (c) Absorptivity spectrum providing narrow band peak absorption at 6.5 µm

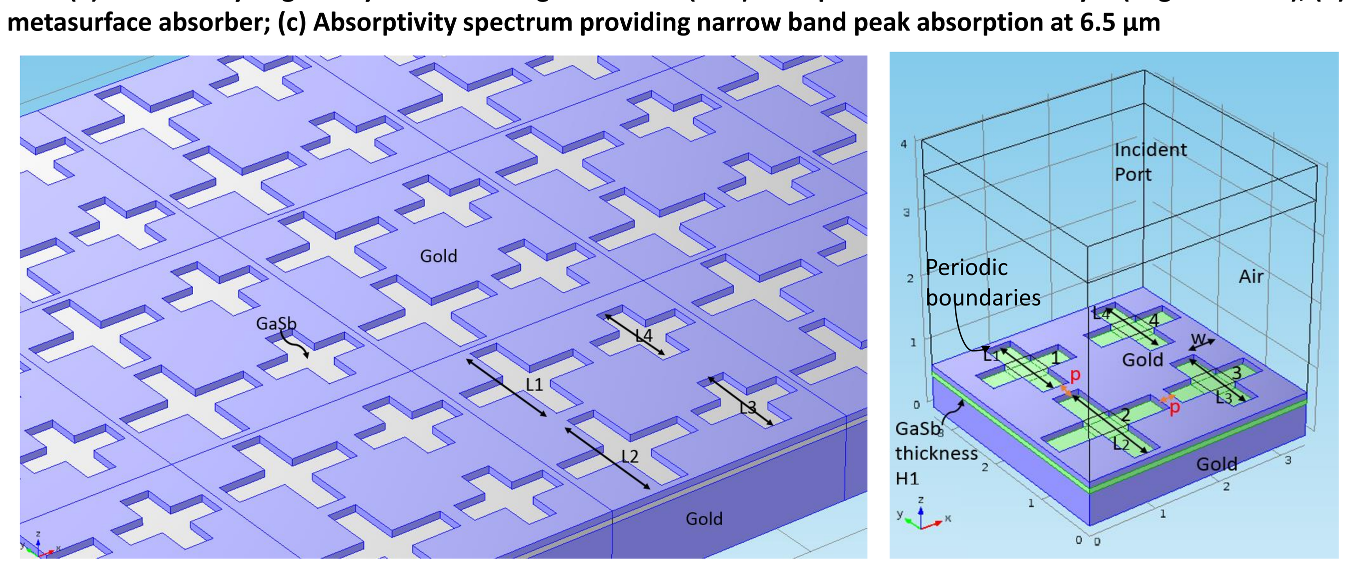

Figure 6. New metasurface design combining four unit cells of the previous design and

In many applications, however, more than one perfect absorption band is required. Based on this motivation, we aim to attain multiband perfect light absorber by combining different sizes of cross-shaped electric ring resonators (ERR) on one plane. To verify this concept, four sub-wavelength cross-shaped electric ring resonators (ERR) are assembly together as a basic compartment filling the entire surface. The resulting metamaterial is illustrated in figure 6 as a metal ERR array with four different characteristic sizes stacked on a thin dielectric material placed on a metal block. We selected gallium antimonide as the material of the dielectric layer to easily achieve peak absorption around 2 µm. Figure 7 shows a good combination of sizes of the ERR and the thickness of the GaAs layer to provide three separated absorption bands with a peak absorption around 1.8 µm. Following the similar approach, we have obtained a continuous broadband perfect light absorber between 0.8 and 1.5 µm when 12 different sizes of ERR are applied in the design of the metasurface.

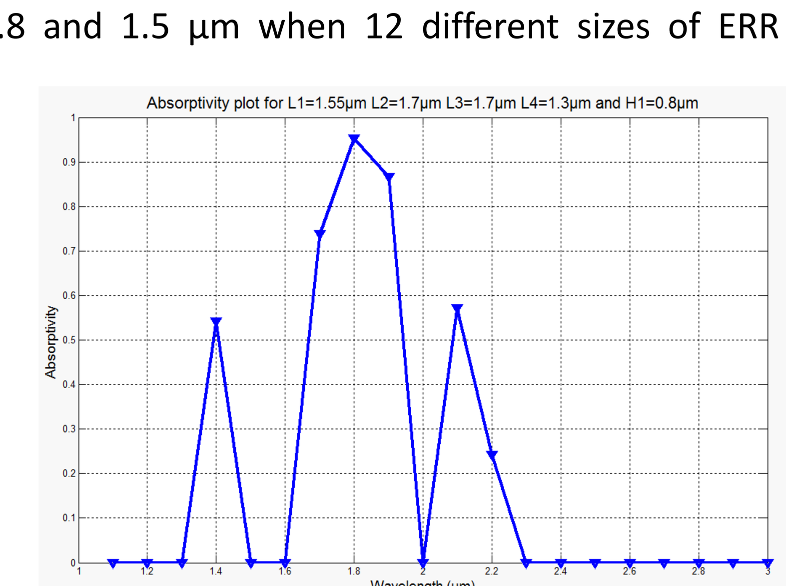

Figure 7. spectral absorptivity (from 1 µm to 2.8 µm) of the resulting metamaterial

Acknowledgement & Notes

The research is supported by NSF CBET-1545546 and Air Force summer faculty fellowship program (2016). We also appreciate for the High Performance Research Computing of TAMU to provide the required computational resources.

All the presented results are accomplished with COMSOL 5.1 and lab-made multiphase two-temperature modules on Ada cluster of TAMU. Each light induced vapor bubble formation simulation requires 4 nodes with 20 CPUs each with a total simulation time less than 48 hours. Each parametric sweep simulation for the design of multiband perfect light absorbers requires 10 nodes with 10 CPUs each with a total simulation time of 72 hours.